THE ZIRCON-REIDITE SHOCK TRANSFORMATION: A TEM STUDY OF REIDITE PRODUCED AT A NEWLY ESTABLISH 21.2 GPa SHOCK PRESSURE THRESHOLD. R. Christoffersen[1], T. M. Erickson[1], C. J. Cline[1], M. J. Cintala[2] and N. E. Timms[3], [1]Jacobs-JETS II contract, NASA Johnson Space Center, 2224 Bay Area Boulevard, Houston, TX, 77058, USA (roy.christoffersen-1@nasa.gov), [2]Astromaterials Research and Exploration Science division, NASA JSC, XI3, 2101 NASA Parkway, Houston, TX, 77058, USA, [3]Space Science and Technology Center, School of Earth and Planetary Science, GPO Box 1984, Perth, WA, 6845, Australia.

Introduction: The high-pressure polymorph of zircon (Zr_2SiO_4) is reidite, a phase with the scheelite structure that was first discovered to form at ca. 12 GPa in static high-pressure experiments [1]. Reidite was subsequently found to occur in naturally shocked zircons from several terrestrial impact localities [2,3], as well as in shock recovery-reverberation experiments performed above 20 GPa [4]. The nature and distribution of reidite occurrences in terrestrial impact localities has pointed to its potential use as a shock pressure indicator, as well as to the importance of understanding its age-reset effects in zircon geochronology [3].

In this study we have used coordinated SEM/Electron Backscatter Diffraction (EBSD) and Field-Emission Scanning Transmission Electron Microscopy (FE-STEM) to study the micro- and nano-structure of reidite and its shocked zircon host produced at 21.2 GPa under experimental shock recovery/reverberation conditions [5]. Our results document the TEM microstructure of reidite formed at a 21.2 GPa experimental shock pressure that is significantly lower than that observed in previous studies [4]. At these conditions the sample developed a diverse set of microstructures that have not been previously documented on the TEM scale.

Experimental and Analytical Methods: Shock reverberation experiments were performed at 18.2 and 21.2 GPa on cm-size oriented single-crystals of Mudtank zircon [6] using the flat-plate accelerator (FPA) at NASA Johnson Space Center (JSC) [5]. The 18.2 and 21.2 GPa samples were cut normal to [001] and {hkl} and loaded into a tungsten-alloy sample container surrounded by randomly oriented zircon powder. Zircon fragments were extracted from the FPA sample container, mounted in epoxy and polished for SEM/EBSD analysis with sub-50 µm colloidal silicate

SEM/EBSD analysis was performed at NASA JSC using a JEOL 7600F field-emission SEM outfitted with an Oxford Instruments Symmetry EBSD detector that also included capabilities for transmitted Kikuchi diffraction (TKD) imaging. Based on SEM/EBSD findings a region in the 21.2 GPa sample was prepared for follow-up TKD and FE-STEM study by focused ion beam (FIB) cross-sectioning using an FEI Quanta Dual-Beam SEM/FIB instrument at NASA JSC. FE-STEM characterization utilized the JEOL 2500SE analytical FE-STEM at NASA JSC. Imaging techniques included both conventional and STEM bright-field (BF)/dark-field (DF) diffraction contrast imaging, and high-resolution lattice fringe imaging (HRTEM).

Results: Our previously reported EBSD findings for the 18.2 and 21.2 GPa samples found oriented microfractures and crystal-plastic deformation bands in the 18.2 GPa sample but did not detect reidite [5]. EBSD of the 21.2 GPa sample found the same oriented microfractures as the 18.2 GPa sample, but also found prominent cross-cutting lamellar features, 1-20 µm-wide, composed of reidite [5]. TKD phase maps of the 21.2 FIB sample also detected reidite in the lamellar features, but found its distribution in the lamellae to be inhomogeneous and mixed with identified zircon regions.

A bright-field STEM image of the 21.2 GPa FIB section is shown in Fig. 1. The FIB section revealed a wide distribution in the widths of the lamellar regions, the largest being ~3 µm wide (Fig. 1), but also many 100-500 nm wide lamellae that were not detected by EBSD/TKD mapping at the SEM scale. Although most of the lamellae share a sub-parallel orientation, many of the narrower lamellae form closely-spaced complex *en-echelon* sets, or are slightly curvilinear.

The 3 µm-wide lamellar region in the FIB section (arrows; Fig. 1) contains a 300 nm-wide layer of single

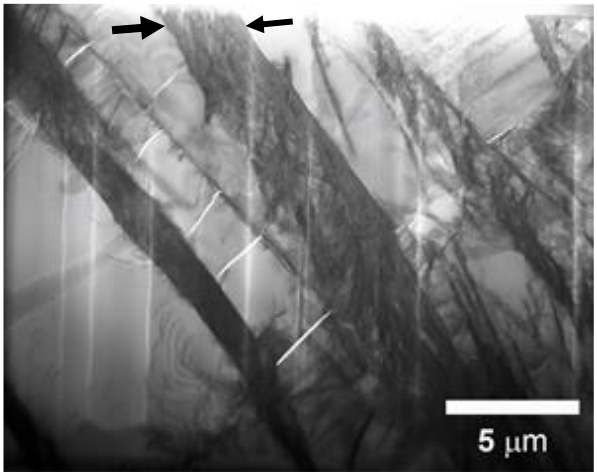

Fig. 1. STEM BF Image of FIB section of 21.2 GPa sample. Arrows show layer described in Fig. 2.

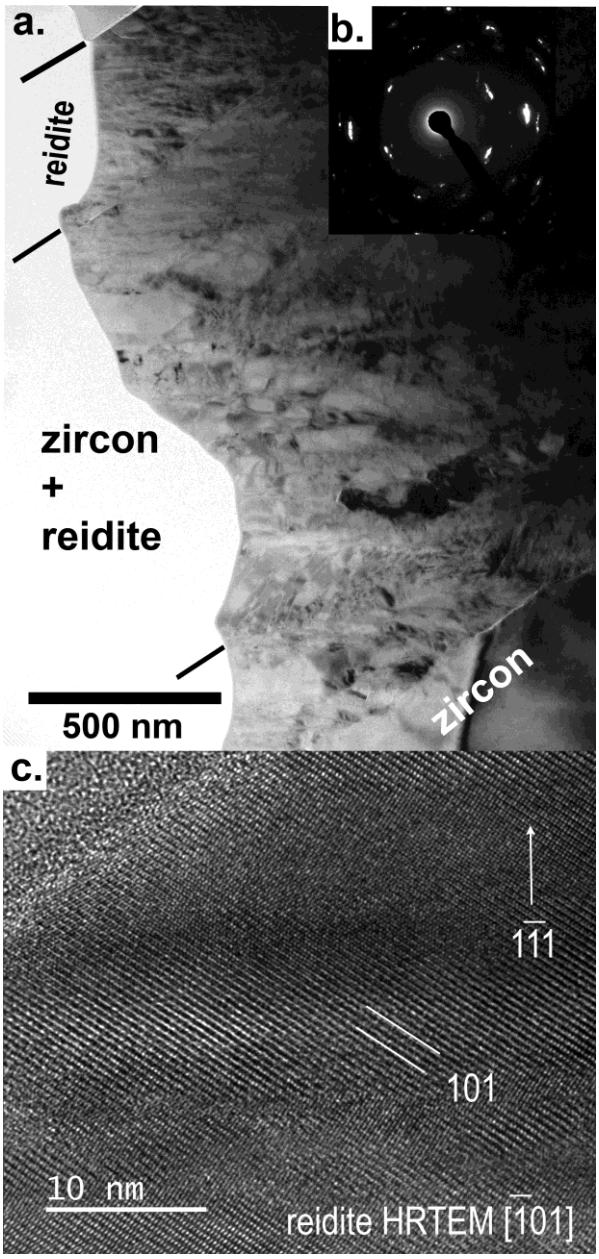

Fig. 2. (a) CTEM BF Image of widest lamellar region in FIB section of 21.2 GPa sample (b) SAED pattern of polycrystalline zircon layer (c) [-101] HRTEM image of reidite single-crystal layer in (a).

crystalline reidite along the lamellar margin in contact with the host single-crystal zircon (Fig. 2a). The rest of the region is a polycrystalline assemblage of zircon grains 20-50 nm in size (Fig. 2a). Selected area electron diffraction (SAED) patterns of this assemblage had no indexable reidite reflections (Fig. 2b). The patterns show limited 10-20º of streaking asterism indicating the zircon grains in the assemblage are crystallographically oriented (Fig. 2b). This preferred orientation was confirmed in CTEM DF imaging, which showed the zircon grains to be arrayed in oriented, elongate single-crystalline domains. Each domain exhibited dense strain contrast associated with regularly spaced sub-grain walls oriented perpendicular to long axis of the grain. The numerous narrower 100-500 nm wide lamellar features in the FIB sample tended to microstructurally resemble the polycrystalline portion of the widest layer, being composed of nm-sized, highly defective zircon crystals. Likewise, the limited set SAED patterns we obtained from these narrower layers did not contain indexable reidite reflections, and HRTEM images did not show reidite lattice fringes.

HRTEM images of the single-crystalline reidite layer in the ~3 µm-wide lamellar region exhibit a wavy contrast modulation oriented normal to the 1-11 reciprocal lattice direction. The modulation is associated with regularly spaced crystallographic boundaries that we suspect may be inclined {112} nanotwins as found in [2].

Discussion: Our FE-STEM imaging and diffraction results corroborate our previous EBSD identification of reidite within the shock-deformed lamellar regions of the 21.2 GPa sample. It is not necessarily a given, however, that all these lamellar regions contain enough reidite to consistently show up in SAED patterns or HRTEM images. The lamellar regions are rather more characterized as zones of concentrated brittle-plastic deformation of the host zircon, in which the deformed zircon microstructure and grain orientation suggests a strong shear component. More detailed study is needed to fully determine the presence or absence of reidite in these nm-scale lamellar regions. The consistent indexing of reidite in EBSD phase maps of the widest (10-30 µm) lamellae at the SEM scale, and localization of well-formed single-crystalline reidite to the widest lamellar region in the TEM FIB sample suggests these wider lamellae may define zones of more efficient reidite formation, possibly due to higher localized shear deformation.

References: [1] Reid A. F. and Ringwood A. E. (1969) EPSL, 6, 205-208. [2] Glass B. P. et al. (2002) *Am. Min.*, 87, 562-565. [3] Erickson T. M. et al. (2017) *Con. Min. Pet.*, 172. [4] Leroux H. et al. (1999) *EPSL, 169*, 291 – 301. [5] Erickson T. M. et al. (2020) *51st LPSC, Abstract #1581*. [6] Black L. P. & Gulson B. L. (1978) *J. of Aus. Geo. and Geophys*. 3, 277 – 232.